JACS
JOURNAL OF THE AMERICAN CHEMICAL SOCIETY

Article

pubs.acs.org/JACS

Integrating Enzymatic Self-Assembly and Mitochondria Targeting for Selectively Killing Cancer Cells without Acquired Drug Resistance

Huaimin Wang,[†,‡] Zhaoqianqi Feng,[†] Youzhi Wang,[‡] Rong Zhou,[†] Zhimou Yang,*[,‡] and Bing Xu*[,†]

[†]Department of Chemistry, Brandeis University, 415 South Street, Waltham, Massachusetts 02453, United States

[‡]State Key Laboratory of Medicinal Chemical Biology, Key Laboratory of Bioactive Materials, Ministry of Education, College of Life Sciences, Collaborative Innovation Center of Chemical Science, Nankai University, Tianjin 300071, P.R. China

Supporting Information

ABSTRACT: Targeting organelles by modulating the redox potential of mitochondria is a promising approach to kill cancer cells that minimizes acquired drug resistance. However, it lacks selectivity because mitochondria perform essential functions for (almost) all cells. We show that enzyme-instructed self-assembly (EISA), a bioinspired molecular process, selectively generates the assemblies of redox modulators (e.g., triphenyl phosphinium (TPP)) in the pericellular space of cancer cells for uptake, which allows selectively targeting the mitochondria of cancer cells. The attachment of TPP to a pair of enantiomeric, phosphorylated tetrapeptides produces the precursors (L-**1P** or D-**1P**) that form oligomers. Upon dephosphorylation catalyzed by ectophosphatases (e.g., alkaline phosphatase (ALP)) overexpressed on cancer cells (e.g., Saos2), the oligomers self-assemble to form nanoscale assemblies only on the surface of the cancer cells. The cancer cells thus uptake these assemblies of TPP via endocytosis, mainly via a caveolae/raft-dependent pathway. Inside the cells, the assemblies of TPP-peptide conjugates escape from the lysosome, induce dysfunction of mitochondria to release cytochrome *c*, and result in cell death, while the controls (i.e., omitting TPP motif, inhibiting ALP, or removing phosphate trigger) hardly kill the Saos2 cells. Most importantly, the repeated stimulation of the cancers by the precursors, unexpectedly, sensitizes the cancer cells to the precursors. As the first example of the integration of subcellular targeting with cell targeting, this study validates the spatial control of the assemblies of nonspecific cytotoxic agents by EISA as a promising molecular process for selectively killing cancer cells without inducing acquired drug resistance.

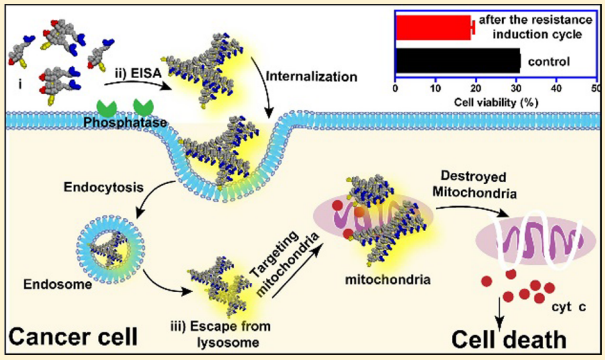

INTRODUCTION

Molecular-targeted therapeutics, which are mostly based on ligand−receptor interactions or enzyme inhibition of a specific target, have been a key strategy for developing anti-cancer drugs. However, recent advances in cancer biology have revealed the great complexity of cancers,[1] such as redundant signaling pathways,[2] acquired drug resistance,[3] genomic instability,[4] intratumoral heterogeneity,[5] and tumor microenvironment.[6] These conceptual advances not only elucidate the mechanism of the drug resistance of the current chemotherapy that aims at only one or two molecular targets (e.g., enzymes, receptors, or transcription factors) but also underscore an urgent need for new approaches for cancer therapy. In contrast to targeting a specific enzyme or protein, targeting a subcellular organelle or antagonizing an essential protein in an organelle represents a unique approach for killing cancer cells[7] without inducing drug resistance. Because the release of cytochrome *c* (cyt c) from mitochondria is a major event in the intrinsic cell death signaling pathway,[8,9] targeting mitochondria[10,11] (e.g., modulating the redox potential of mitochondria[12]) to induce the death of cancer cells may be advantageous over the specific ligand−receptor interaction in countering drug resistance in cancer therapy.[10]

Since the report by Murphy et al. that triphenyl phosphinium (TPP) is a facile molecular motif for targeting the mitochondrial matrix,[13] considerable research activities have focused on targeting mitochondria.[14,15] For example, attachment of bioactive molecules or therapeutic agents to TPP is the most facile and explored strategy,[15] which endows the resulting molecules with targeting and enhanced activity, even against drug-resistant cancer.[16] One prominent example is gamitrinib, an HSP90 inhibitor designed to target the mitochondria of human cancer cells[17] because of the essential role of HSP90 in the survival of cancer cells.[18] A similar strategy was also applied to other anti-cancer drugs which show activity in mitochondria.[15,19] Besides TPP, mitochondria-penetrating peptides are another promising type of candidates explored for modulating the intracellular distribution of bioactive molecules.[20] Although these preclinical studies indicate that targeting an organelle (e.g., mitochondria) or a nodal protein (e.g., HSP90) in multiple signaling networks is a promising approach for killing cancer cells without inducing drug resistance, such approaches

Received: September 18, 2016
Published: November 14, 2016

DOI: 10.1021/jacs.6b09783
J. Am. Chem. Soc. 2016, 138, 16046−16055

still suffer drawbacks and remain to be improved because these organelles or nodal proteins also are critical components of the functions of normal cells. Moreover, if the antagonist of a nodal protein is based on specific ligand−receptor interaction, drug resistance still may emerge due to the mutation of the receptors. Therefore, it is still necessary to develop novel approaches that are multiple-targeting and minimize the emergence of drug resistance.[21]

To achieve multi-targeting, high selectivity, and minimal drug resistance, we chose to combine mitochondria targeting with cell targeting. We use TPP for mitochondria targeting and enzyme-instructed self-assembly (EISA) for cell targeting. As a bioinspired,[22] multiple-step molecular process[23,24] that integrates enzymatic reaction and self-assembly,[25−27] EISA is emerging as a promising strategy for targeting cancer cells.[28] Specifically, we conjugate TPP with a tetrapeptide derivative that undergoes EISA. The tetrapeptide consists of a self-assembling motif as the backbone, being phosphorylated on tyrosine and capped at the N-terminal by a fluorophore. Attaching TPP to the ε-amine of the lysine residue on the tetrapeptide forms the precursors (L-**1P** and D-**1P**), while replacing TPP by acetyl at the ε-position generates L-**2P** and D-**2P** as the controls. Upon dephosphorylation of the precursors by alkaline phosphatase (ALP), the resulting products self-assemble to form nanoscale assemblies via non-covalent interactions, as evidenced by static light scattering (SLS) and transmission electron microscopy (TEM).

Most importantly, L-**1P** or D-**1p** selectively kills human osteosarcoma cells (Saos2) while being innocuous to normal cells (HS5). D-**1P**, being more stable inside cells, is more potent than L-**1P**. L-**2P** or D-**2P**, even at 10 times concentration of L-**1P** or D-**1P**, shows no toxicity to Saos2 cells, confirming cytotoxicity from the TPP. Moreover, Saos2 cells, after being incubated with L-**1P** (or D-**1P**) for 5 weeks with a stepwise increase in the concentration of L-**1P** (or D-**1P**), show little acquired drug resistance to L-**1P** or (D-**1P**). Unexpectedly, the treated cells become more sensitive to the assemblies of TPP. Our preliminary mechanistic study reveals that L-**1** or D-**1**, after being generated via in situ dephosphorylation of L-**1P** or D-**1P**, respectively, being up-taken by the cancer cells (mainly via caveolae/raft-dependent endocytosis, plus clathrin-mediated endocytosis in some extent), and escaping from lysosome, localizes on mitochondria. The assemblies of L-**1** or D-**1** disrupt the homeostasis of mitochondria, trigger the release of cyt c, activate caspase cascade,[8,29] and result in cancer cell death. As the first case of integration of cell and subcellular targeting processes, this work demonstrates a new strategy to selectively kill cancer cells via targeting an organelle in a cell-specific manner. Moreover, this work illustrates a new method for the uptake of self-assembled short peptides and the effective release of the load from endosomes and lysosomes, which can be useful for designing enzyme-instructed systems to promote the endocytosis of drug candidates that fail due to poor cell uptake.

RESULTS AND DISCUSSION

Molecule Design and Synthesis. Figure 1 shows the representative structure of the molecules designed for integrating EISA with mitochondria targeting. The molecules consist of four key features: a self-assembling backbone (i.e., a tetrapeptide, Phe-Phe-Tyr-Lys (FFYK)), an enzymatic trigger (i.e., tyrosine phosphate ($_p$Y) as a substrate of ALP), an environment-sensitive fluorophore (4-nitro-2,1,3-benzoxadiazole

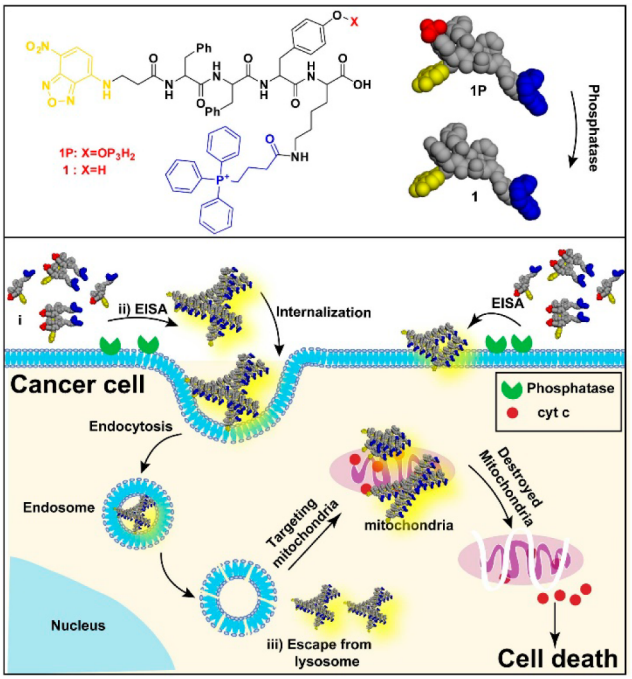

Figure 1. Illustration of enzyme-instructed self-assembly for targeting mitochondria and inducing death of cancer cell.

(NBD)), and a mitochondria targeting motif (i.e., TPP). We choose FFYK because tyrosine provides a facile way to introduce the enzymatic triggers and FFY has acted as a motif for EISA.[30] We use NBD because NBD is a sensitive fluorophore for reporting molecular self-assembly in cellular milieu.[31] We utilize TPP because TPP is an efficient and well-established molecule for targeting the mitochondrial matrix.[32] To understand the effect of stability and stereochemistry of the peptides on the activity of the designed molecules, we use both L-amino acid residues and D-amino acid residues to form the tetrapeptidic backbone. Such a design gives L-**1P** and D-**1P** as the precursors, and L-**1** and D-**1** as the self-assembling molecules. We also use acetyl group to replace TPP to generate L-**2P** and D-**2P** as the controls of L-**1P** and D-**1P**, respectively. Based on the design shown in Figure 1, the cancer cells that overexpress ALP would generate the assemblies of the TPP-conjugates selectively on the cancer cells so that TPP only targets the mitochondria of cancer cells. We also expect NBD, as an imaging probe, to help reveal the dynamic of the TPP assemblies during and after EISA of the TPP-conjugates on the cancer cells.

Scheme 1 shows a facile and general procedure for synthesizing the designed molecules. After using one step reaction of amine active NBD-Cl with β-alanine to produce NBD-β-alanine in over 90% yield and using 9-fluorenylmethoxycarbonyl (Fmoc) to protect phosphorylated tyrosine,[33] we subsequently synthesize NBD-FF$_p$YK (L or D enantiomer) by standard solid-phase (Fmoc) peptide chemistry.[34] After *N*-hydroxysuccinimide (NHS) activates the carboxyl group of TPP, TPP-NHS ester reacts with NBD-FFpYK via ε-amino group of lysine to form stable amide bonds to result in L-**1P** or D-**1P**. Instead of TPP-NHS ester, the use of acetic anhydride to react with ε-amine of lysine produces the control precursors of L-**2P** and D-**2P** in a similar way (Scheme 1). After purifying all the precursors by high-performance liquid chromatography (HPLC), we use ^{1}H NMR and LC-MS to confirm their purity and identity.

DOI: 10.1021/jacs.6b09783
J. Am. Chem. Soc. 2016, 138, 16046−16055

Scheme 1. Structures and Synthetic Route of the Precursors Containing Phosphotyrosine and TPP, and the Control Molecules

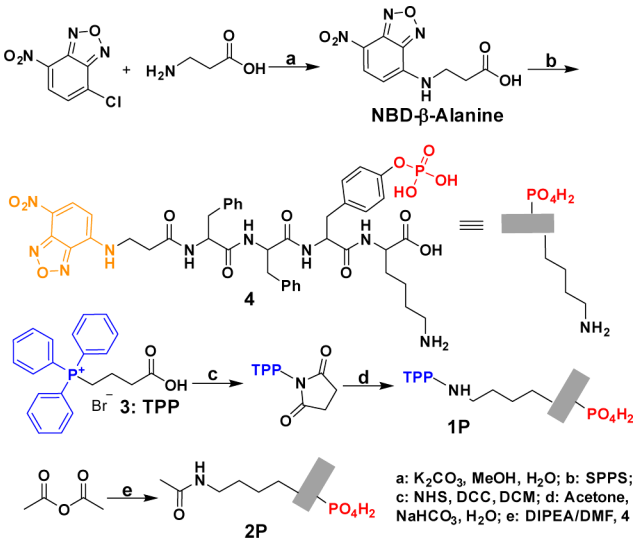

Enzymatic Self-Assembly in Vitro. After obtaining all the precursors, we evaluate their behaviors for EISA in vitro by using TEM and SLS to examine the nanostructures formed before and after the addition of ALP into the solutions of the precursors. After drying from solution, L-**1P** (50 μM) shows many tiny nanoparticles with diameter of 5 ± 2 nm, which tend to aggregates to result in irregular fibrous structures with diameter of 7 ± 2 nm (Figure S1), while at higher concentration, L-**1P** (100 μM) mainly forms irregular fibrous structure with few of oligomers (Figure S2 and S3). As a contrast, D-**1P** (50 μM) forms slightly more regular fibrous structures with diameter of 8 ± 2 nm, which then interact with each other to form dense 2D/3D networks. Interestingly, D-**1P** (100 μM) forms more uniform nanoparticles with diameter of 25 ± 2 nm (Figure S2). As revealed by the dephosphorylation experiment (Figure S4), D-**1P** undergoes ALP-catalyzed dephosphorylation slightly faster than L-**1P** does, with $t_{1/2}$ = 0.55 and 1.14 h for D-**1P** and L-**1P**, respectively, when the substrates is 0.1 wt% and ALP is 0.1 U/mL. After 24 h, the percentages of enzymatic dephosphorylation of D-**1P** and L-**1P** are about 90% and 80%, respectively. The percentage of conversion changes a little with prolonged incubation, suggesting that the nanostructures formed mainly by L-**1** (or D-**1**) likely incorporate the precursors to hinder their complete dephosphorylation. After being formed by dephosphorylation, L-**1** and D-**1** form different nanostructures. TEM indicates that, after being generated by treating L-**1P** with ALP (1 U/mL), L-**1** (50 μM) forms vesicles that interact with each other strongly, which gives hollow colloids with a mean diameter of 79 ± 2 nm and the thickness of 4 ± 2 nm. Similar to L-**1**, D-**1** forms aggregated hollow colloids with a larger mean diameter (106 ± 2 nm) and slightly thicker layers (thickness of 6 ± 2 nm). Dynamic light scattering (DLS) shows the size distribution of L-1P (D-1P) without or with the addition of ALP (1U/mL) in phosphate-buffered saline (PBS) buffer (Figure S5). At the concentration of 100 μM, the size of L-1P (or D-1P) is 121 nm (or 58 nm), and increases to 635 nm (or 196 nm) after the treatment of ALP; at the concentration of 50 μM, the size of L-1P (or D-1P) is 56 nm (or 67 nm), and increases to 198 nm (or 139 nm) after the addition of ALP. Due to solvation, the sizes of the aggregates measured by DLS are larger than that observed in TEM. L-**2P** or D-**2P** (50 μM) forms amorphous aggregates after dissolve in PBS buffer (pH = 7.4) (Figure S6). While the addition of ALP converts L-**2P** to L-**2** to form uniform nanofibers with diameter of 9 ± 2 nm, the enzymatic conversion of D-**2P** to D-**2** results in nanoscale aggregates with diameter of 16 ± 2 nm. These results suggest that the TPP motif likely causes the morphology of the nanostructures of **L-1P**/D-**1P** to differ significantly from those of L-**2P**/D-**2P**. As a charged, steric-hindered motif being connect to the tetrapeptide via a relatively flexible linker, TPP disrupts intermolecular packing to disfavor the formation of long nanofibers, but it promotes interparticle interaction to favor polymorphic aggregates before and after enzymatic dephosphorylation. Such a plasticity of the assemblies of small molecules may be useful to reduce the acquired drug resistance if the assemblies are cytotoxicity species (vide infra).

To further evaluate the self-assembly properties of precursors before and after the addition of ALP, we also use SLS to examine the signal changes of the precursor before and after the enzymatic dephosphorylation (Figure 2). The solution of

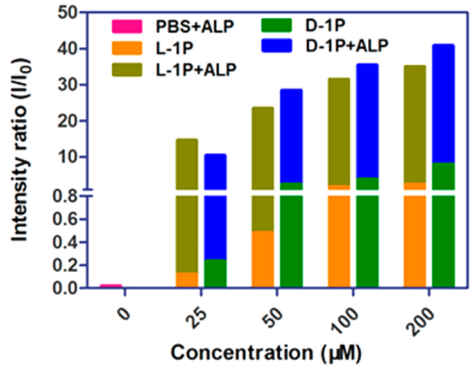

Figure 2. Intensity of static light scattering of the solutions of L-**1P** and D-**1P** (25–200 μM) before and after addition of alkaline phosphatase (1 U/mL) for 24 h at different concentrations in phosphate-buffered saline buffer (pH 7.4).

L-**1P** (or D-**1P**) exhibits enhanced signal with the increase of concentration (from 25 μM to 200 μM). This result indicates that both precursors are able to form aggregates in some extent, agreeing with the results of TEM. After the addition of ALP to the solution of each precursor, the SLS signal increases significantly, up to more than 10-fold. Depending on the initial concentrations of the precursors, the increase of the SLS signals for L-**1P** is 120-fold (25 μM), 48-fold (50 μM), 18-fold (100 μM) and 14-fold (200 μM), while that for D-**1P** is 43-fold (25 μM), 10-fold (50 μM), 8-fold (100 μM), and 4-fold (200 μM). These results confirm that L-**1P** and D-**1P** are excellent precursors for EISA based on ALP.

Cytotoxicity and Selectivity. To investigate the cellular response of all the precursors, we first use 3-(4,5-dimethylthiazol-2-yl)-2,5-diphenyltetrazolium bromide (MTT)[35] assay to examine the viability of human osteosarcoma cells (Saos2, which expresses high level ALP[36]) cultured with the precursors. As a control, we also examine the viability of normal human bone marrow stromal cells (HS5) that express low level of ALP on cell surface.[24] As shown in Figure 3, L-**1P** exhibits IC_{50} of 61 ± 2 μM (76.1 ± 2.5 μg/mL, 48h) against Saos2 cells in a dosage-dependent manner. D-**1P** exhibits IC_{50} of 46 ± 2 μM (57.4 ± 2.5 μg/mL, 48h), lower than the IC_{50} of L-**1P**.

DOI: 10.1021/jacs.6b09783
J. Am. Chem. Soc. 2016, 138, 16046–16055

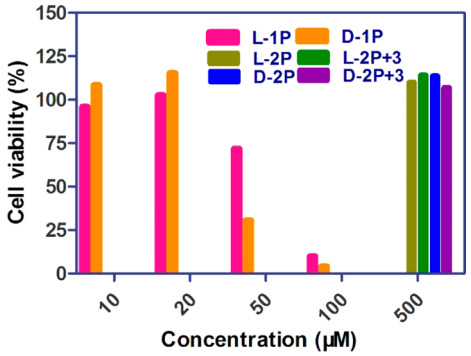

Figure 3. Cell viability of Saos2 cells after being incubated with L-**1P**, D-**1P**, L-**2P**, D-2P, L-**2P**+3, or D-**2P**+3 for 48 h.

In the presence of exogenous ALP, L-**1P** (or D-**1P**) turns into L-**1** (or D-**1**), which is innocuous to Saos2 cells at the concentrations up to 200 μM (Figure S14). This result confirms that L-**1** (or D-**1**), if not being generated in situ on the cancer cell surface, is innocuous to the cells. As another control, L-**2P** (or D-**2P**) by itself or being co-incubated with the targeting motif TPP (**3**) hardly exhibits cytotoxicity against Saos2 cell, even at 500 μM. This result suggests that the conjugation of TPP to the self-assembling tetrapeptide is necessary for the observed cytotoxicity. To investigate the retention of L-**1** (or D-**1**) in the Saos2 cells, we incubate Saos2 cells with L-**1P** (D-**1P**, 50 μM) for different times. The result (Figure S8) indicates that the intracellular concentration of L-**1** increases at first 6 h, and decreases with the longer incubation time. In contrast, the concentration of D-**1** decreases little after 6 h incubation. Moreover, the intracellular concentration of D-**1** is 3.5-fold of that of L-**1** at 6 h incubation, but the ratio increases to 10-fold at 24 h incubation. This result agrees with the proteolytic stability of D-**1**, which is consistent with the higher cytotoxicity of D-**1P** than that of L-**1P**.

We also examine the cytotoxicity of L-**1P** and D-**1P** against HS5 cells. Our results indicate that L-**1P** (or D-**1P**) is almost innocuous to HS5 cells at 100 μM, the concentrations that kill over 90% of Saos2 cells (Figures S7 and S9). To evaluate whether the precursors inhibit other cancer cell lines that express low levels of ALPs, we incubate L-**1P** (or D-**1P**) with HeLa (human cervical adenocarcinoma cell line), HepG2 (human liver carcinoma cell line), T98G (glioblastoma multiforme tumor cell line), and MCF7 (human breast adenocarcinoma cell line). Expressing lower level of ALPs on their cell surfaces than on Saos2 cell surface, these cells are less susceptible than Saos2 cell to L-**1P** (or D-**1P**). That is, the IC_{50} of L-**1P** (or D-**1P**) against these cells are higher than 200 μM (Figure S10). At 200 μM, L-**1P** and D-**1P**, exhibit similar cytotoxicities against HeLa, HepG2 or MCF7 cells at 48h (Figure S9). Interestingly, D-**1P** is less cytotoxic than L-**1P** against T98G cells. This difference may originate from the difference in stereochemistry and may deserve further investigation in future work. These results, together with TEM and SLS results, indicate that the integration of cell targeting (by EISA) and mitochondria targeting (by TPP) is an efficient strategy for selectively inhibiting the cancer cells that express high level of ALP.[37]

Escaping from Lysosome and Targeting Mitochondria. We next use confocal laser scanning microscopy (CLSM) to examine the intracellular localization of L-**1** and D-**1** in Saos2 cells. As shown in Figure 4, most of the green fluorescent dots

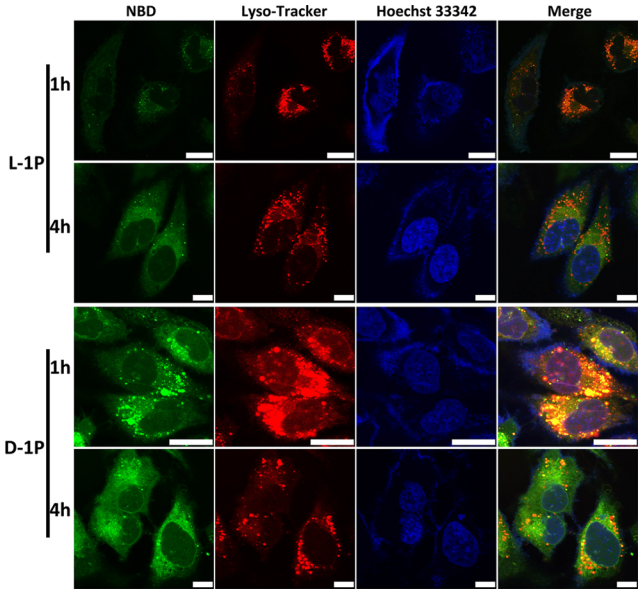

Figure 4. CLSM images of Saos2 cells treated with L-**1P** or D-**1P** (50 μM) for 1 or 4 h and then stained with Lyso-Tracker. Scale bar is 10 μm.

(belonging to NBD of L-**1** or D-**1** in the Saos2 cells) co-localize with the red dots (belonging to Lyso-Tracker[38]) within 1 h, suggesting the uptake of L-**1** (or D-**1**) by cells via endocytosis.[39] However, there is little overlap of the fluorescence between green (NBD) and red (Lyso-Tracker) signals after 4 h incubation, indicating that the assemblies of L-**1** (or D-**1**) escape from late endosome/lysosome into cytosol. Fluorescent imaging (Figure S11) also shows that the hydrogelators (L-**1** or D-**1**) present in the divided cells (from the second to the fourth passage), suggesting that L-**1** or D-**1** likely escapes partially from the endosome/lysosomes. The escape of tetrapeptidic derivatives from endosome/lysosome, to the best of our knowledge, is the first report of such phenomenon.[40]

To further evaluate the cellular distribution of L-**1** (or D-**1**) after its in situ formation, we also use Mito-Tracker to co-stain with all the precursors.[41] As shown in Figure 5, the green fluorescence signal from NBD also co-localizes well with the red fluorescence signal from the Mito-Tracker in the cytosol after co-incubation for 4 h. Moreover, the green fluorescence on the cell surface indicates that the assemblies of L-**1** (or D-**1**) not only enter the cell to target mitochondria, but also self-assemble on cell surface, as demonstrated by 3D construction of confocal images (see SI Video 1 and Video 2). These results suggest that L-**1P** (or D-**1P**) induces cancer cell death likely via three key processes (Figure 1): (i) L-**1P** (or D-**1P**) itself forms oligomers at certain concentration, which then interact with each other to form nanoscale assemblies. (ii) ALPs on the Saos2 cell surface, being expressed in high level, catalyze the rapid dephosphorylation of L-**1P** (or D-**1P**) for generating of L-**1** (or D-**1**) (i.e., EISA occurs on the cancer cell surface[42]). The process of EISA further induces the assemblies of L-**1** (or D-**1**) on cell surface, which then are internalized by the cancer cells through endocytosis. (iii) The internalized assemblies of L-**1** (or D-**1**) escape from late endosome/lysosome, then target mitochondria because of TPP. Unlike monomeric TPP that rescues cells,[43] the assemblies (or aggregates) of the TPP-tetrapeptide conjugate function as multivalent TPPs, which enhance the disruption of the mitochondria. That is, the

DOI: 10.1021/jacs.6b09783
J. Am. Chem. Soc. 2016, 138, 16046−16055

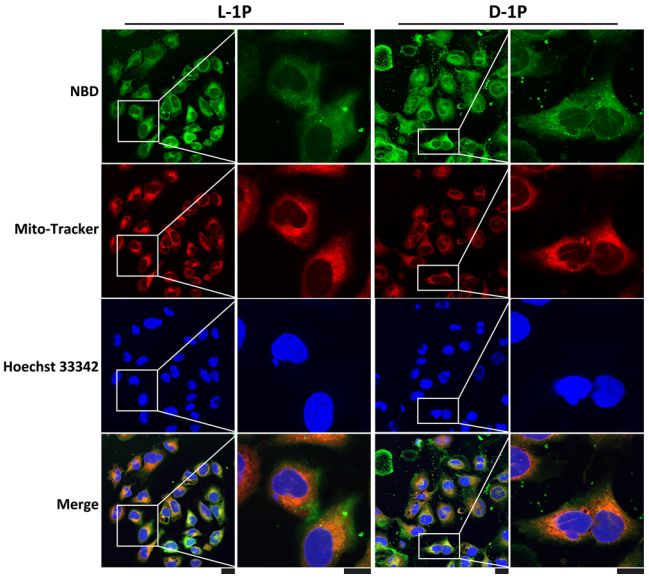

Figure 5. Confocal laser scanning microscopy images of Saos2 cells treated with L-**1P** or D-**1P** (50 μM) for 4 h, and then stained with Mito-tracker. Scale bar for low magnification is 25 and for higher magnification is 15 μm.

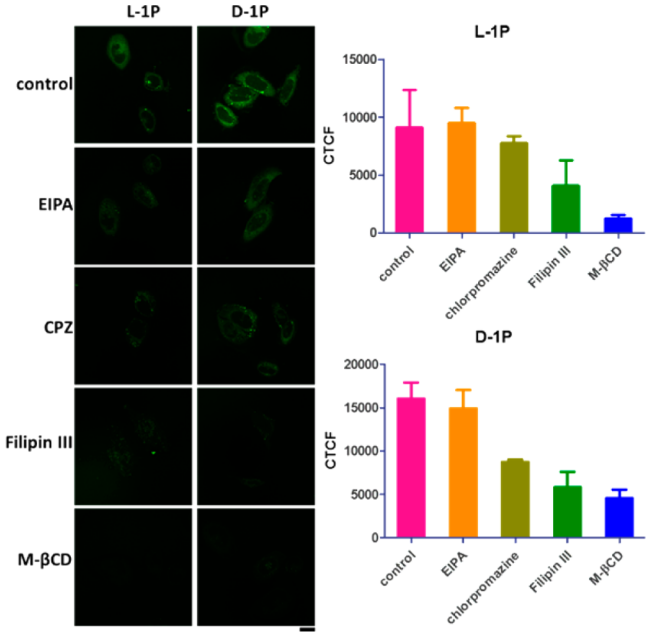

Figure 6. CLSM images (green represent the fluorescence of NBD at excitation of 488 nm) and the corrected total cell fluorescence (CTCF, quantified from the gray scale of CLSM images) of Saos-2 cells treated with L-**1P** or D-**1P** (50 μM) for 1 h in the absence (control) or presence of the inhibitors EIPA (100 μM, ethyl-isopropyl-amiloride), CPZ (30 μM, chlorpromazine), Filipin III (5 μg/mL), and M-βCD (5 mM). Scale bar is 15 μm.

dynamic transport of the assemblies on cell surface to the surface of mitochondria, ultimately, kills the cancer cells. Because HS5 expresses low levels of ALP, L-**1P** (or D-**1P**) is inefficient for undergoing EISA, thus L-**1P** (or D-**1P**) exhibits little toxicity to HS5 cells.

Modes of Endocytosis. To examine the modes of endocytosis that involve the uptake of the TPP-peptide conjugates by the Saos2 cells, we incubate the Saos2 cells with L-**1P** (or D-**1P**, 50 μM) at 4 °C because all endocytic pathways are energy-dependent processes that slow down at low temperature.[44] As revealed by the results of co-localization experiment, L-**1P**/L-**1** (or D-**1P**/D-**1**) hardly enters the cells or associates with cell membranes at 4 °C (Figure S12), confirming that the internalization of L-**1** (or D-**1**) is energy-dependent. To determine which kinds of endocytotic process being responsible for the uptake, we use several well-established endocytotic inhibitors to co-incubate with L-**1P** (or D-**1P**) in the culture of Saos2 cells. As shown in Figure 6, the addition of 5-(*N*-ethyl-*N*-isopropyl)-amiloride (EIPA), an inhibitor of macropinocytosis and phagocytosis in most mammalian cells,[45] hardly affects the uptake of L-**1** (or D-**1**). The addition of chlorpromazine (CPZ), one of cationic amphipathic drug that inhibits clathrin-mediated endocytosis,[46] reduces the uptake of L-**1** for about 15% and D-**1** for about 45% (according to the quantification of intracellular fluorescence of NBD obtained by CLSM). The additions of Filipi III and M-βCD, inhibitors of lipid raft/caveolae-mediated endocytosis,[47] significantly affect the uptake of L-**1** and D-**1**. Specifically, Filipin III reduces the uptake of L-**1** and D-**1** for about 55% and 64%, respectively. M-βCD reduces the uptake of L-**1** and D-**1** for about 86% and 72%, respectively. These results indicate that, after being generated by the dephosphorylation of L-**1P** (or D-**1P**), the assemblies of L-**1** or D-**1** mainly undergo caveolae/lipid raft-mediated endocytosis,[48] plus certain extent of clathrin-mediated endocytosis.[49]

Mechanism of Cell Death. To demonstrate the essential role of EISA for its anti-cancer activities, we co-incubate the precursor and the ALP inhibitors during cell viability experiment. We use three kinds of established ALP inhibitors: L-phenylalanine (L-Phe),[50] an efficient uncompetitive inhibitor of placental alkaline phosphatase (PLAP); levamisole, a well-known uncompetitive inhibitor of tissue-nonspecific alkaline phosphatase (TNAP);[50] and CinnGEL 2Me,[51] an inhibitor of protein tyrosine phosphatase (PTP1B) that localizes at the cytoplasmic face of the endoplasmic reticulum. As shown in Figure 7A (and Figure S14), co-incubating the precursors with L-Phe or CinnGEL 2Me hardly rescues the Saos2 cells, while levamisole increases the cell viability of Saos2 cells treated by L-**1P** or D-**1P** (even at the concentration as high as 200 μM). To be specific, the cell viability of Saos2 cells in the presence of L-**1P** or D-**1P**, respectively, increases from 21.6% or 11.5% to 65.3% or 66.0% at the concentration of 100 μM for 48 h, and from 2.1% or 1.8% (indicating that almost all the cells are dead) to 50.5% or 53.3% at the concentration of 200 μM for 48 h. These results are consistent with the expression levels of isoforms of ALPs on Saos2 cells, which express more TNAP than PLAP on the cell surface.[27,52] Moreover, the PTP1B inhibitor (i.e., CinnGEL 2Me) is unable to rescue the cells, supporting the mechanism in Figure 1 that EISA on the cell surface is the key processes for converting L-**1P** and D-**1P** to L-**1** and D-**1**, respectively. To further confirm the critical role of ALPs on cell surface, we incubate the precursors together with ALP, which serves as an exogenous enzyme. The addition of ALP almost eliminates the cytotoxicity of the precursors. Thus, these results suggest that the process of EISA on cell surface plays an important role for the activity of the precursors, which further influence the uptake of the assemblies of L-**1** or D-**1**.

To understand how the process of EISA on cell surface influences the uptake of L-**1** (or D-**1**), we use confocal microscope to detect the uptake of L-**1** (or D-**1**) in the presence of different inhibitors of ALPs. As shown in Figure 7B (and Figures S15 and S16), Saos2 cells exhibit similar fluorescence

DOI: 10.1021/jacs.6b09783
J. Am. Chem. Soc. 2016, 138, 16046−16055

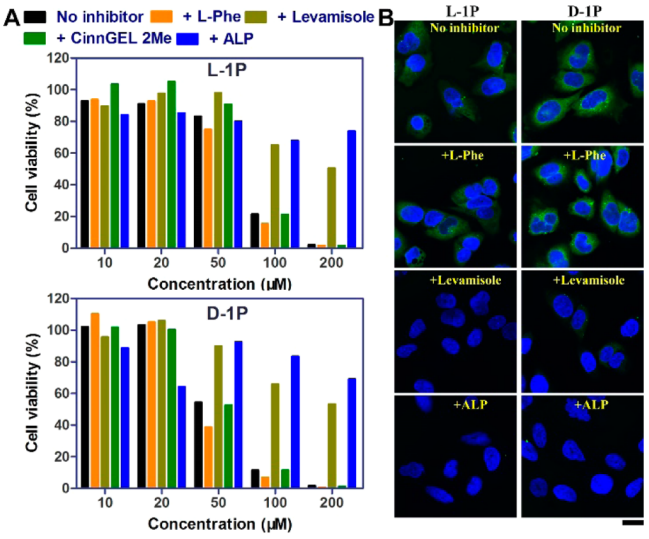

Figure 7. (A) Cell viability of Saos2 cell line treated by L-**1P** or D-**1P** (50 μM) in the presence of phosphatase inhibitors or exogenous ALP for 48 h. (B) CLSM images (green represent the fluorescence of NBD at excitation of 488 nm and blue represent the fluorescence of Hoechst 3342 to stain cellular nucleus) of Saos2 cells treated with L-**1P** or D-**1P** (50 μM) for 4 h in the absence or with phosphatase inhibitors or exogenous ALP. Scale bar is 10 μm. [L-Phe] = [levamisole] = 1 mM, CinnGEL 2Me = 2 μM, [ALP] = 10 U/mL.

without and with the presence of L-Phe, indicating that L-Phe hardly hinders the uptake of L-**1** (or D-**1**). This result agrees that most of the ALPs on Saos2 are TNAPs. On the contrary, cells treated by the precursors with levamisole or exogenous ALPs show much weaker fluorescence than the control cells (only being incubated with the precursors). These results, therefore, confirm that the EISA, as a process, is critical for the uptake of L-**1** (or D-**1**). In other words, when the inhibitor of ectoenzyme (TNAPs) or the presence exogenous ALPs blocks or disrupts the process of EISA, the precursors are unable to turn into the assemblies of L-**1** or D-**1** on the cancer cell surface, thus further hampering the uptake of the aggregates, so Saos2 cells remain viable, as shown in the MTT assay (Figures 7A and S14). This detailed exploration of EISA on Saos2 cell surface also illustrates a way of modulating EISA on other cells for controlling the behavior of the cells.

The endocytotic mechanism of the assemblies of L-**1** (or D-**1**) and the presence of some fluorescence puncta on the Saos2 cell surface (Figure 5) prompt us to examine the changes of cytoskeleton of the Saos2 cells. We use Alexa Fluor 633 phalloidin,[53] which specifically stains the actin cytoskeleton, to reveal the changes of actin filament. As shown in Figure 8, the actin filaments in the control Saos2 cells (untreated cells (Ctr)) exhibit well-arranged parallel structures with long and thick fibers. After the cells being treated with L-**1P** (or D-**1P**) for 1 h at the concentration of 100 μM, some of the actin filaments become disorganized, aggregating into short and ill-defined fibers and puncta. In addition, there are more puncta in the cells treated by D-**1P** than in those treated by L-**1P**. These results suggest that the impaired actin cytoskeletons, caused by aggregates of L-**1** (or D-**1**), contribute to the cell death. This observation implies that EISA on the cell surface not only is the key process for the subcellular targeting of mitochondria by the aggregates formed by L-**1** (or D-**1**), but also is one of the key contributions for interacting with the cytoskeleton, which likely influences the dynamic of cell

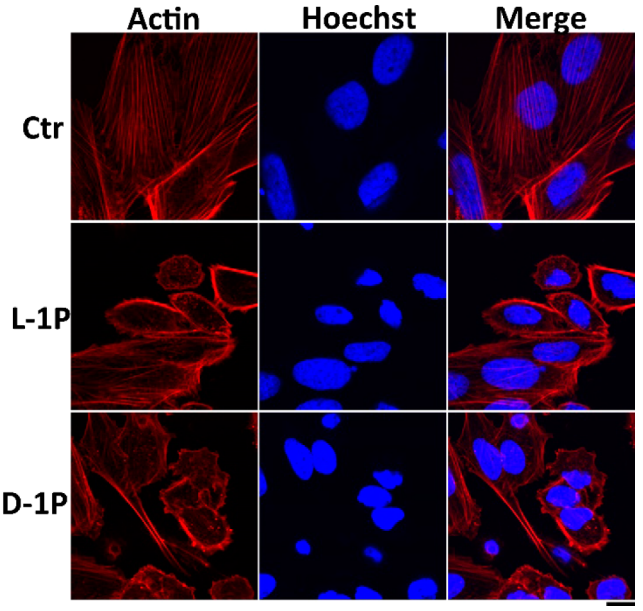

Figure 8. CLSM images of Saos2 cells stained with Alexa Fluor 633 phalloidin (F-actin, red) and Hoechst (nuclei, blue) without or with the addition of L-**1P** or D-**1P** (100 μM) for 1 h. Scale bar is 15 μm.

membrane, enhances the uptake of aggregates, and results in effective anti-cancer activity.

Modality of Cell Death. To evaluate the modality of cell death induced by L-**1P** (or D-**1P**), we first co-incubate a pan-caspase inhibitor (zVAD-fmk)[54] or a necroptosis inhibitor (Nec-1)[55] with the precursors in the culture of the Saos2 cells. As shown in Figure 9 (Figure S17), zVAD-fmk (45 μM), which

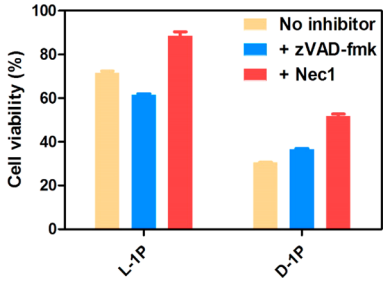

Figure 9. Cell viability of Saos2 cells treated by L-**1P** or D-**1P** (50 μM) in the presence of cell death signaling inhibitors at 48 h ([zVAD-fmk] = 45 μM, [Nec-1] = 50 μM).

itself shows no toxicity on Saos2 cells, hardly rescues the cells but exhibits a little more toxicity when being co-incubate with L-**1P** (50 μM) for 48 h. However, it can rescue Saos2 cells when it co-incubates with D-**1P**. Notably, Nec-1 can reduce the toxicity of L-**1P** (or D-**1P**) to some extent. These results indicate that L-**1P** (or D-**1P**) induces cell death involving more necroptosis than apoptosis. Since Nec-1 is unable to rescue the cells fully, other mechanisms likely also contribute the death of Saos2 induced by the addition of L-**1P** (or D-**1P**).

Apoptotic Signaling Induced by the Assemblies of L-1 (or D-1). To gain insight into the mechanism of Saos2 cell death induced by L-**1P** (or D-**1P**), we use PathScan apoptosis multi-target sandwich ELISA to detect the changes of endogenous level of key signaling proteins in pathways controlling survival and apoptosis.[56] As shown in Figure 10, the expression level of phosphorylated p53 decreases a little in

DOI: 10.1021/jacs.6b09783
J. Am. Chem. Soc. 2016, 138, 16046−16055

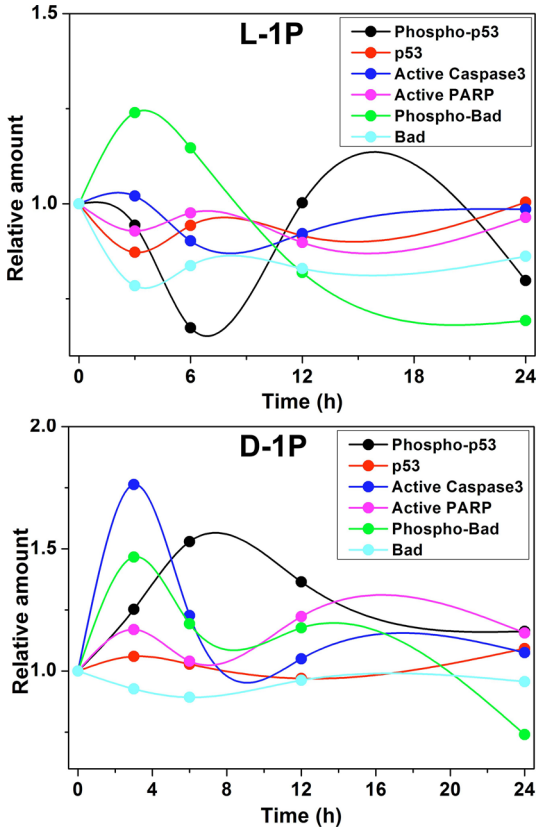

Figure 10. Time-dependent activation of apoptotic proteins of Saos2 cell treated with L-**1P** or D-**1P** (50 μM).

the first 6 h and increases after 12 h of incubation of L-**1P**, while the Saos2 cells treated with D-**1P** express a high level of phosphorylated p53 with extended incubation time to 8 h. The expression level of phosphorylated p53 decreases to a constant amount for the next 8 h. The expression level of active caspase3 is significantly different between the Saos2 cells treated with L-**1P** and D-**1P**. Active caspase3 changes little when L-**1P** treating the Saos2 cells, but it increases to about 1.7-fold at first 3 h treatment of D-**1P**, and then decreases to the constant amount that is same as the untreated cells. Interestingly, the expression of active-PARP or Bad remains almost constant in the treatment of L-**1P** (or D-**1P**), while the expression level of phosphorylated Bad increases and reaches a high level at an incubation time of 3 h, and drops quickly with the extended time of incubation. Since Bad is a proapoptotic member of the Bcl-2 family,[57] the decreased expression level of phosphorylated Bad indicate that Bad is activated by dephosphorylation under stress, which then activates the apoptotic effector machinery, and triggers the release of cyt c from mitochondria to cytosol[58] (vide infra).

Release of Cytochrome *c* to the Cytosol. Based on the CLSM experiment (Figure 5), which indicates that L-**1** (D-**1**) can interact with and enrich in the cellular mitochondria, and that the modality of cell death (Figures 9 and 10) depends on intrinsic apoptosis in some extent, we assume that the cell death induced by L-**1P** (or D-**1P**) involves the release of cyt c, an essential component of the mitochondrial respiratory chain,[12,59] from mitochondria to cytosol. To confirm this hypothesis, we prepare the cytosol from the Saos2 cells according to an established method[60] in the presence of 50 μM L-**1P** (or D-**1P**) and use time-dependent Western blot to detect the

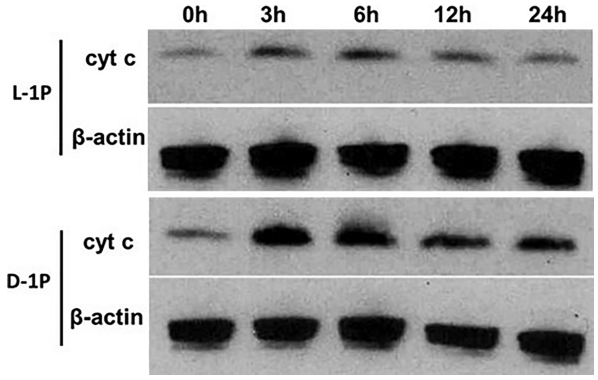

Figure 11. Time-dependent Western blot analysis of cytochrome *c* from the cytosolic fraction of Saos2 cells treated with L-**1P** or D-**1P** (50 μM).

expression levels of cyt c at different time incubation. As shown in Figure 11, the cyto c in the cytosol significantly increases at first 6 h in the presence of L-**1P** (or D-**1P**), and remains in the cytosols in the test period of 24 h. Moreover, the expression level of cyt c in the presence of D-**1P** is higher than in the presence of L-**1P**, indicating D-**1P** is more efficient than L-**1P** for modulating the homeostasis of mitochondria on Saos2 cells. This result agrees with the cytotoxicity of L-**1P** (or D-**1P**, Figure 3). As a control, we also prepare the whole-cell fraction (containing both cytosol and mitochondria) of Saos2 cells treated with L-**1P** (or D-**1P**), the time-dependent Western blot indicates that the cyt c in the fraction of whole cell remains constant (Figure S18). These results indicate that assemblies of L-**1** (or D-**1**), formed by EISA, result in dysfunction of mitochondria of the Saos2 cells, which release cyt c to the cytosol to activate the caspase cascade signaling pathway, thus triggering intrinsic apoptosis of the Saos2 cells[61] as one of the modes of the death of the Saos2 cells.

L-1P (or D-1P) Causes No Acquired Drug Resistance. Based on the above mechanism of cell death showing that L-**1P** (or D-**1P**) activates multiple death signaling pathways, we reckon that cancer cells unlikely would be able to evolve resistance toward this multiple targeting strategy. Moreover, the assemblies of L-**1** (or D-**1**), unlike traditional small molecule inhibitors, are plastic (i.e., exhibiting polymorphism). Such a plasticity should minimize the path to drug resistance. Thus, we examine whether Saos2 cells can evolve acquired resistance after being repeatedly stimulated by L-**1P** (or D-**1P**) at suboptimal concentrations, which is an established method to select drug resistant cancer cells.[62] We incubate the precursors with Saos2 cells by gradually increasing the concentration of L-**1P** (or D-**1P**) from 10 to 50 μM for 5 weeks and select the cells that survive the treatment. After that, we test the selected Saos2 cells with L-**1P** (or D-**1P**) by MTT assay. As shown in Figure 12, the IC_{50} of L-**1P** against Saos2 cells (after 5 weeks stimulation of L-**1P**) is 36.8 μM for 48 h, and the IC_{50} of D-**1P** is 35.2 μM against Saos2 cells (after 5 weeks stimulation of D-**1P**), which is similar to the previous results of cytotoxicities of the D-**1P** on the unstimulated Saos2 cells. Surprisingly, the repeated stimulation of Saos2 cells significantly sensitizes the Saos2 cells to the assemblies of L-**1**: at 50 μM of L-**1P**, the cell viability of unstimulated Saos2 is 71.7%, but it drops to 20.5% for the selected cells. While this observation deserves further mechanistic exploration in future study, these preliminary results, undoubtedly, indicate that multiple targeting (cell and subcellular targetings) is a promising strategy

DOI: 10.1021/jacs.6b09783
J. Am. Chem. Soc. 2016, 138, 16046−16055

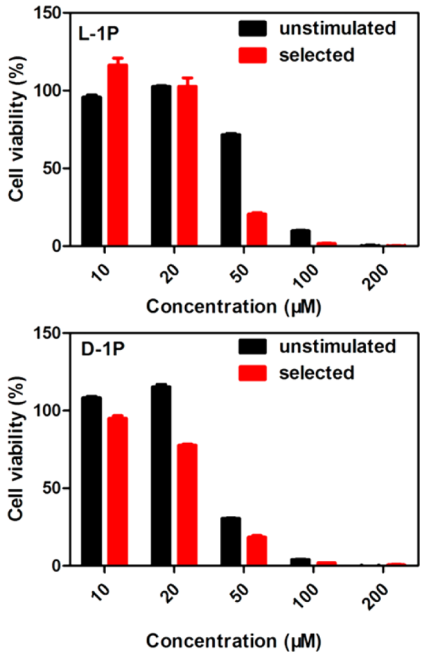

Figure 12. Cell viability of unstimulated Saos2 cell line or selected Saos2 cell line (after 5 weeks treatment of the precursors with gradually increase concentrations) incubated with L-**1P** or D-**1P** at different concentrations for 48 h.

for minimizing acquired drug resistance. Since the biggest challenge in cancer therapy and drug discovery is drug resistance,[63] this result indicates that combining EISA with other targeting strategy to generate anti-cancer supramolecular assemblies promises a fundamentally new direction for anti-cancer drug discovery.

CONCLUSION

In summary, we report the first case of integrating cell and subcellular targeting for selectively killing cancer cells without causing acquired drug resistance. By rationally designing the precursors consisting of a peptide segment of EISA and a mitochondria-targeting motif, testing the precursors in cell assays, and preliminarily examining the mechanisms of cellular uptake and cell death, we validate the concept of using the molecular process for multi-targeting. Moreover, stimulating the Saos2 cells by the precursors hardly induces acquired resistance. As anti-cancer drug resistance remains the challenge for most modern drug discovery and the reason for the failure of most clinical drugs (e.g., cisplatin, doxorubicin),[64] the strategy demonstrated in this work promises more profound impacts than just killing the Saos2 cells. In addition, the use of the enantiomer pairs (i.e., L-**1P** and D-**1P**) to treat the same set of cells, undoubtedly, validates the molecular processes and targets involving in the cell death of the cancer cells. The concept demonstrated here should be applicable for designing the precursors as the substrates of other enzymes overexpressed by cancer cells[65] (e.g., CD73,[66] MMP9,[26,67] and furin[68]) and other subcellular organelle.[69] Although the concentration required for killing cells is relatively high according current clinical standard based on highly potent yet unselective drugs (e.g., cisplatin), the exceptional selectivity exhibit by the precursors (i.e., L-**1P** and D-**1P**) may still achieve acceptable therapeutic index, which remains to be confirmed. Nevertheless, this strategy, combining cell targeting and subcellular targeting, promises a new way to counter anti-cancer drug resistance. Currently, we are engineering the molecules for achieve high activity against cancer cells and tuning the distribution of bioactive molecules.[70]

ASSOCIATED CONTENT

Supporting Information

The Supporting Information is available free of charge on the ACS Publications website at DOI: 10.1021/jacs.6b09783.

Materials and detailed experimental procedures; Figures S1−S25 (PDF)

Video 1, 3D construction of confocal images of Saos2 cells treated with L-**1P** (AVI)

Video 2, 3D construction of confocal images of Saos2 cells treated with D-**1P**(AVI)

AUTHOR INFORMATION

Corresponding Authors

*yangzm@nankai.edu.cn

*bxu@brandeis.edu

ORCID

Huaimin Wang: 0000-0002-8796-0367

Zhimou Yang: 0000-0003-2967-6920

Bing Xu: 0000-0002-4639-387X

Notes

The authors declare no competing financial interest.

ACKNOWLEDGMENTS

This work was partially supported by NIH (R01CA142746), Keck Foundation, NSF (MRSEC-1420382), and International S&T Cooperation Program of China (ISTCP, 2015DFA50310)

REFERENCES

(1) Hanahan, D.; Weinberg, R. A. *Cell* **2011**, *144*, 646.

(2) Stommel, J. M.; Kimmelman, A. C.; Ying, H.; Nabioullin, R.; Ponugoti, A. H.; Wiedemeyer, R.; Stegh, A. H.; Bradner, J. E.; Ligon, K. L.; Brennan, C.; et al. *Science* **2007**, *318*, 287. Thornberry, N. A.; Rano, T. A.; Peterson, E. P.; Rasper, D. M.; Timkey, T.; Garcia-Calvo, M.; Houtzager, V. M.; Nordstrom, P. A.; Roy, S.; Vaillancourt, J. P.; et al. *J. Biol. Chem.* **1997**, *272*, 17907.

(3) Hayes, J. D.; Pulford, D. J. *Crit. Rev. Biochem. Mol. Biol.* **1995**, *30*, 521.

(4) Campbell, P. J.; Yachida, S.; Mudie, L. J.; Stephens, P. J.; Pleasance, E. D.; Stebbings, L. A.; Morsberger, L. A.; Latimer, C.; McLaren, S.; Lin, M.-L.; et al. *Nature* **2010**, *467*, 1109. Negrini, S.; Gorgoulis, V. G.; Halazonetis, T. D. *Nat. Rev. Mol. Cell Biol.* **2010**, *11*, 220.

(5) Patel, A. P.; Tirosh, I.; Trombetta, J. J.; Shalek, A. K.; Gillespie, S. M.; Wakimoto, H.; Cahill, D. P.; Nahed, B. V.; Curry, W. T.; Martuza, R. L.; et al. *Science* **2014**, *344*, 1396. Campbell, L. L.; Polyak, K. *Cell Cycle* **2007**, *6*, 2332.

(6) Mantovani, A.; Allavena, P.; Sica, A.; Balkwill, F. *Nature* **2008**, *454*, 436. Vaupel, P.; Kallinowski, F.; Okunieff, P. *Cancer Res.* **1989**, *49*, 6449.

(7) Murphy, M. P. *Biochim. Biophys. Acta, Bioenerg.* **2008**, *1777*, 1028.

(8) Liu, X.; Kim, C. N.; Yang, J.; Jemmerson, R.; Wang, X. *Cell* **1996**, *86*, 147.

(9) Luo, X.; Budihardjo, I.; Zou, H.; Slaughter, C.; Wang, X. *Cell* **1998**, *94*, 481.

(10) Kang, B. H.; Plescia, J.; Dohi, T.; Rosa, J.; Doxsey, S. J.; Altieri, D. C. *Cell* **2007**, *131*, 257.

(11) Chevalier, A.; Zhang, Y.; Khdour, O. M.; Kaye, J. B.; Hecht, S. M. *J. Am. Chem. Soc.* **2016**, *138*, 12009.

(12) Green, D. R.; Reed, J. C. *Science* **1998**, *281*, 1309.

(13) Burns, R. J.; Smith, R. A. J.; Murphy, M. P. *Arch. Biochem. Biophys.* **1995**, *322*, 60.
(14) Yasueda, Y.; Tamura, T.; Fujisawa, A.; Kuwata, K.; Tsukiji, S.; Kiyonaka, S.; Hamachi, I. *J. Am. Chem. Soc.* **2016**, *138*, 7592. Zha, J.; Weiler, S.; Oh, K. J.; Wei, M. C.; Korsmeyer, S. J. *Science* **2000**, *290*, 1761. Weinberg, S. E.; Chandel, N. S. *Nat. Chem. Biol.* **2015**, *11*, 9. Wang, J.-X.; Jiao, J.-Q.; Li, Q.; Long, B.; Wang, K.; Liu, J.-P.; Li, Y.-R.; Li, P.-F. *Nat. Med.* **2011**, *17*, 71.
(15) Fulda, S.; Galluzzi, L.; Kroemer, G. *Nat. Rev. Drug Discovery* **2010**, *9*, 447.
(16) Armstrong, J. *Br. J. Pharmacol.* **2007**, *151*, 1154. Marrache, S.; Pathak, R. K.; Dhar, S. *Proc. Natl. Acad. Sci. U. S. A.* **2014**, *111*, 10444.
(17) Kang, B. H.; Plescia, J.; Song, H. Y.; Meli, M.; Colombo, G.; Beebe, K.; Scroggins, B.; Neckers, L.; Altieri, D. C. *J. Clin. Invest.* **2009**, *119*, 454.
(18) Hendrick, J. P.; Hartl, F.-U. *Annu. Rev. Biochem.* **1993**, *62*, 349. Whitesell, L.; Lindquist, S. L. *Nat. Rev. Cancer* **2005**, *5*, 761.
(19) D'Souza, G. G.; Wagle, M. A.; Saxena, V.; Shah, A. *Biochim. Biophys. Acta, Bioenerg.* **2011**, *1807*, 689.
(20) Horton, K. L.; Stewart, K. M.; Fonseca, S. B.; Guo, Q.; Kelley, S. O. *Chem. Biol.* **2008**, *15*, 375. Yousif, L. F.; Stewart, K. M.; Horton, K. L.; Kelley, S. O. *ChemBioChem* **2009**, *10*, 2081. Jean, S. R.; Ahmed, M.; Lei, E. K.; Wisnovsky, S. P.; Kelley, S. O. *Acc. Chem. Res.* **2016**, *49*, 1893.
(21) Wang, H.; Feng, Z.; Wu, D.; Fritzsching, K. J.; Rigney, M.; Zhou, J.; Jiang, Y.; Schmidt-Rohr, K.; Xu, B. *J. Am. Chem. Soc.* **2016**, *138*, 10758−10761.
(22) Whitesides, G. M. *Interface Focus* **2015**, *5*, 20150031.
(23) Zhou, J.; Xu, B. *Bioconjugate Chem.* **2015**, *26*, 987.
(24) Zhou, J.; Du, X.; Berciu, C.; He, H.; Shi, J.; Nicastro, D.; Xu, B. *Chem.* **2016**, *1*, 246.
(25) Yang, Z.; Liang, G.; Xu, B. *Acc. Chem. Res.* **2008**, *41*, 315. Li, X.; Kuang, Y.; Lin, H. C.; Gao, Y.; Shi, J.; Xu, B. *Angew. Chem., Int. Ed.* **2011**, *50*, 9365. Li, X.; Kuang, Y.; Shi, J.; Gao, Y.; Lin, H.-C.; Xu, B. *J. Am. Chem. Soc.* **2011**, *133*, 17513.
(26) Yang, Z.; Ma, M.; Xu, B. *Soft Matter* **2009**, *5*, 2546.
(27) Zhou, J.; Du, X.; Yamagata, N.; Xu, B. *J. Am. Chem. Soc.* **2016**, *138*, 3813.
(28) Yang, Z.; Xu, K.; Guo, Z.; Guo, Z.; Xu, B. *Adv. Mater.* **2007**, *19*, 3152. Pires, R. A.; Abul-Haija, Y. M.; Costa, D. S.; Novoa-Carballal, R.; Reis, R. L.; Ulijn, R. V.; Pashkuleva, I. *J. Am. Chem. Soc.* **2015**, *137*, 576. Tanaka, A.; Fukuoka, Y.; Morimoto, Y.; Honjo, T.; Koda, D.; Goto, M.; Maruyama, T. *J. Am. Chem. Soc.* **2015**, *137*, 770. Huang, P.; Gao, Y.; Lin, J.; Hu, H.; Liao, H.-S.; Yan, X.; Tang, Y.; Jin, A.; Song, J.; Niu, G.; et al. *ACS Nano* **2015**, *9*, 9517.
(29) Li, P.; Nijhawan, D.; Budihardjo, I.; Srinivasula, S. M.; Ahmad, M.; Alnemri, E. S.; Wang, X. *Cell* **1997**, *91*, 479.
(30) Gao, Y.; Kuang, Y.; Guo, Z.-F.; Guo, Z.; Krauss, I. J.; Xu, B. *J. Am. Chem. Soc.* **2009**, *131*, 13576.
(31) Gao, Y.; Shi, J.; Yuan, D.; Xu, B. *Nat. Commun.* **2012**, *3*, 1033. Gao, Y.; Kuang, Y.; Du, X.; Zhou, J.; Chandran, P.; Horkay, F.; Xu, B. *Langmuir* **2013**, *29*, 15191. Zhou, J.; Du, X.; Li, J.; Yamagata, N.; Xu, B. *J. Am. Chem. Soc.* **2015**, *137*, 10040. Gao, Y.; Berciu, C.; Kuang, Y.; Shi, J.; Nicastro, D.; Xu, B. *ACS Nano* **2013**, *7*, 9055.
(32) Smith, R. A.; Porteous, C. M.; Gane, A. M.; Murphy, M. P. *Proc. Natl. Acad. Sci. U. S. A.* **2003**, *100*, 5407.
(33) Ottinger, E. A.; Shekels, L. L.; Bernlohr, D. A.; Barany, G. *Biochemistry* **1993**, *32*, 4354.
(34) Coin, I.; Beyermann, M.; Bienert, M. *Nat. Protoc.* **2007**, *2*, 3247. Wellings, D. A.; Atherton, E. *Methods Enzymol.* **1997**, *289*, 44.
(35) Gerlier, D.; Thomasset, N. *J. Immunol. Methods* **1986**, *94*, 57.
(36) Farley, J. R.; Hall, S. L.; Herring, S.; Tarbaux, N. M.; Matsuyama, T.; Wergedal, J. E. *Metab., Clin. Exp.* **1991**, *40*, 664.
(37) McComb, R. B.; Bowers, G. N., Jr.; Posen, S. *Alkaline phosphatase*; Plenum Press: New York, 1979.
(38) Zhou, R.; Yazdi, A. S.; Menu, P.; Tschopp, J. *Nature* **2011**, *469*, 221.
(39) Subach, F. V.; Subach, O. M.; Gundorov, I. S.; Morozova, K. S.; Piatkevich, K. D.; Cuervo, A. M.; Verkhusha, V. V. *Nat. Chem. Biol.* **2009**, *5*, 118.
(40) Lock, L. L.; Reyes, C. D.; Zhang, P.; Cui, H. *J. Am. Chem. Soc.* **2016**, *138*, 3533.
(41) Shim, S.-H.; Xia, C.; Zhong, G.; Babcock, H. P.; Vaughan, J. C.; Huang, B.; Wang, X.; Xu, C.; Bi, G.-Q.; Zhuang, X. *Proc. Natl. Acad. Sci. U. S. A.* **2012**, *109*, 13978.
(42) Kuang, Y.; Shi, J.; Li, J.; Yuan, D.; Alberti, K. A.; Xu, Q.; Xu, B. *Angew. Chem., Int. Ed.* **2014**, *53*, 8104.
(43) Mukhopadhyay, A.; Weiner, H. *Adv. Drug Delivery Rev.* **2007**, *59*, 729.
(44) Rejman, J.; Oberle, V.; Zuhorn, I. S.; Hoekstra, D. *Biochem. J.* **2004**, *377*, 159. Gump, J. M.; Dowdy, S. F. *Trends Mol. Med.* **2007**, *13*, 443.
(45) Nakase, I.; Niwa, M.; Takeuchi, T.; Sonomura, K.; Kawabata, N.; Koike, Y.; Takehashi, M.; Tanaka, S.; Ueda, K.; Simpson, J. C. *Mol. Ther.* **2004**, *10*, 1011.
(46) Inal, J.; Miot, S.; Schifferli, J. A. *Exp. Cell Res.* **2005**, *310*, 54.
(47) Smart, E. J.; Anderson, R. G. *Methods Enzymol.* **2002**, *353*, 131. Ros-Baró, A.; López-Iglesias, C.; Peiró, S.; Bellido, D.; Palacín, M.; Zorzano, A.; Camps, M. *Proc. Natl. Acad. Sci. U. S. A.* **2001**, *98*, 12050. Monis, G. F.; Schultz, C.; Ren, R.; Eberhard, J.; Costello, C.; Connors, L.; Skinner, M.; Trinkaus-Randall, V. *Am. J. Pathol.* **2006**, *169*, 1939.
(48) Ostrom, R. S.; Insel, P. A. *Br. J. Pharmacol.* **2004**, *143*, 235.
(49) Sigismund, S.; Woelk, T.; Puri, C.; Maspero, E.; Tacchetti, C.; Transidico, P.; Di Fiore, P. P.; Polo, S. *Proc. Natl. Acad. Sci. U. S. A.* **2005**, *102*, 2760.
(50) Borgers, M. *J. Histochem. Cytochem.* **1973**, *21*, 812.
(51) Zhu, S.; Bjorge, J. D.; Fujita, D. J. *Cancer Res.* **2007**, *67*, 10129.
(52) Millán, J. L. *Mammalian alkaline phosphatases: from biology to applications in medicine and biotechnology*; John Wiley & Sons: New York, 2006.
(53) Eiseler, T.; Döppler, H.; Yan, I. K.; Kitatani, K.; Mizuno, K.; Storz, P. *Nat. Cell Biol.* **2009**, *11*, 545.
(54) Slee, E. A.; Zhu, H.; Chow, S. C.; MacFarlane, M.; Nicholson, D. W.; Cohen, G. M. *Biochem. J.* **1996**, *315*, 21.
(55) Degterev, A.; Huang, Z.; Boyce, M.; Li, Y.; Jagtap, P.; Mizushima, N.; Cuny, G. D.; Mitchison, T. J.; Moskowitz, M. A.; Yuan, J. *Nat. Chem. Biol.* **2005**, *1*, 112.
(56) Budihardjo, I.; Oliver, H.; Lutter, M.; Luo, X.; Wang, X. *Annu. Rev. Cell Dev. Biol.* **1999**, *15*, 269. Li, F.; Ambrosini, G.; Chu, E. Y.; Plescia, J.; Tognin, S.; Marchisio, P. C.; Altieri, D. C. *Nature* **1998**, *396*, 580.
(57) Yang, E.; Zha, J.; Jockel, J.; Boise, L. H.; Thompson, C. B.; Korsmeyer, S. J. *Cell* **1995**, *80*, 285.
(58) Tan, Y.; Demeter, M. R.; Ruan, H.; Comb, M. J. *J. Biol. Chem.* **2000**, *275*, 25865. Eskes, R.; Antonsson, B.; Osen-Sand, A.; Montessuit, S.; Richter, C.; Sadoul, R.; Mazzei, G.; Nichols, A.; Martinou, J.-C. *J. Cell Biol.* **1998**, *143*, 217. Shimizu, S.; Narita, M.; Tsujimoto, Y.; Tsujimoto, Y. *Nature* **1999**, *399*, 483.
(59) Kroemer, G.; Reed, J. C. *Nat. Med.* **2000**, *6*, 513.
(60) Dopp, E.; von Recklinghausen, U.; Hartmann, L. M.; Stueckradt, I.; Pollok, I.; Rabieh, S.; Hao, L.; Nussler, A.; Katier, C.; Hirner, A. V.; et al. *Drug Metab. Dispos.* **2008**, *36*, 971.
(61) Kluck, R. M.; Bossy-Wetzel, E.; Green, D. R.; Newmeyer, D. D. *Science* **1997**, *275*, 1132. Yang, J.; Liu, X.; Bhalla, K.; Kim, C. N.; Ibrado, A. M.; Cai, J.; Peng, T.-I.; Jones, D. P.; Wang, X. *Science* **1997**, *275*, 1129.
(62) Cillo, C.; Dick, J.; Ling, V.; Hill, R. *Cancer Res.* **1987**, *47*, 2604. Riganti, C.; Miraglia, E.; Viarisio, D.; Costamagna, C.; Pescarmona, G.; Ghigo, D.; Bosia, A. *Cancer Res.* **2005**, *65*, 516. Riganti, C.; Kopecka, J.; Panada, E.; Barak, S.; Rubinstein, M. *J. Natl. Cancer Inst.* **2015**, *107*, djv046.
(63) Ford, J. M.; Hait, W. N. *Pharmacol. Rev.* **1990**, *42*, 155. Dean, M.; Fojo, T.; Bates, S. *Nat. Rev. Cancer* **2005**, *5*, 275. Brown, J. M.; Giaccia, A. J. *Cancer Res.* **1998**, *58*, 1408.
(64) Hamilton, T. C.; Winker, M. A.; Louie, K. G.; Batist, G.; Behrens, B. C.; Tsuruo, T.; Grotzinger, K. R.; McKoy, W. M.; Young,

DOI: 10.1021/jacs.6b09783
J. Am. Chem. Soc. 2016, 138, 16046−16055

R. C.; Ozols, R. F. *Biochem. Pharmacol.* **1985**, *34*, 2583. Gottesman, M. M. *Annu. Rev. Med.* **2002**, *53*, 615.
(65) Hirst, A. R.; Roy, S.; Arora, M.; Das, A. K.; Hodson, N.; Murray, P.; Marshall, S.; Javid, N.; Sefcik, J.; Boekhoven, J.; et al. *Nat. Chem.* **2010**, *2*, 1089. Komatsu, H.; Shindo, Y.; Oka, K.; Hill, J. P.; Ariga, K. *Angew. Chem., Int. Ed.* **2014**, *53*, 3993.
(66) Wu, D.; Du, X.; Shi, J.; Zhou, J.; Zhou, N.; Xu, B. *J. Colloid Interface Sci.* **2015**, *447*, 269.
(67) Kalafatovic, D.; Nobis, M.; Javid, N.; Frederix, P. W.; Anderson, K. I.; Saunders, B. R.; Ulijn, R. V. *Biomater. Sci.* **2015**, *3*, 246. Lin, Y.-A.; Ou, Y.-C.; Cheetham, A. G.; Cui, H. *Biomacromolecules* **2014**, *15*, 1419. Huang, Y.; Shi, J.; Yuan, D.; Zhou, N.; Xu, B. *Biopolymers* **2013**, *100*, 790.
(68) Liang, G.; Ren, H.; Rao, J. *Nat. Chem.* **2010**, *2*, 54. Ye, D.; Shuhendler, A. J.; Cui, L.; Tong, L.; Tee, S. S.; Tikhomirov, G.; Felsher, D. W.; Rao, J. *Nat. Chem.* **2014**, *6*, 519. Miao, Q.; Bai, X.; Shen, Y.; Mei, B.; Gao, J.; Li, L.; Liang, G. *Chem. Commun.* **2012**, *48*, 9738.
(69) Ferri, K. F.; Kroemer, G. *Nat. Cell Biol.* **2001**, *3*, E255. Kiyonaka, S.; Kajimoto, T.; Sakaguchi, R.; Shinmi, D.; Omatsu-Kanbe, M.; Matsuura, H.; Imamura, H.; Yoshizaki, T.; Hamachi, I.; Morii, T.; et al. *Nat. Methods* **2013**, *10*, 1232. Ishida, M.; Watanabe, H.; Takigawa, K.; Kurishita, Y.; Oki, C.; Nakamura, A.; Hamachi, I.; Tsukiji, S. *J. Am. Chem. Soc.* **2013**, *135*, 12684.
(70) Feng, Z.; Wang, H.; Du, X.; Shi, J.; Li, J.; Xu, B. *Chem. Commun.* **2016**, *52*, 6332.

DOI: 10.1021/jacs.6b09783
J. Am. Chem. Soc. 2016, 138, 16046−16055